

RED CELLS, IRON, AND ERYTHROPOIESIS

Iron homeostasis governs erythroid phenotype in polycythemia vera

Cavan Bennett,^{1,2} Victoria E. Jackson,^{1,2} Anne Pettikiriarachchi,¹ Thomas Hayman,¹ Ute Schaeper,³ Gemma Moir-Meyer,^{1,2} Katherine Fielding,^{1,2,4} Ricardo Ataide,^{1,5} Danielle Clucas,^{1,2,4} Andrew Baldi,^{1,2} Alexandra L. Garnham,^{2,6} Connie S. N. Li-Wai-Suen,^{2,6} Stephen J. Loughran,^{7,8} E. Joanna Baxter,^{7,8} Anthony R. Green,^{7,8} Warren S. Alexander,^{2,9} Melanie Bahlo,^{1,2} Kate Burbury,¹⁰ Ashley P. Ng,^{2,9,10} and Sant-Rayn Pasricha^{1,2,4,10}

¹Population Health and Immunity Division, Walter and Eliza Hall Institute of Medical Research, Parkville, VIC, Australia; ²Department of Medical Biology, University of Melbourne, Parkville, VIC, Australia; ³Silence Therapeutics GmbH, Berlin, Germany; ⁴Diagnostic Haematology, The Royal Melbourne Hospital, Parkville, VIC, Australia; ⁵Department of Infectious Diseases, Peter Doherty Institute, University of Melbourne, Parkville, VIC, Australia; ⁶Bioinformatics Division, Walter and Eliza Hall Institute of Medical Research, Parkville, VIC, Australia; ⁷Wellcome–MRC Cambridge Stem Cell Institute, Jeffrey Cheah Biomedical Centre and ⁸Department of Haematology, University of Cambridge, Cambridge, United Kingdom; ⁹Blood Cells and Blood Cancer Division, Walter and Eliza Hall Institute of Medical Research, Parkville, VIC, Australia; and ¹⁰Clinical Haematology at the Peter MacCallum Cancer Centre and The Royal Melbourne Hospital, Melbourne, VIC, Australia

KEY POINTS

- **Homozygous *HFE* mutations are overrepresented in patients with PV.**
- **Hepcidin levels govern severity of, and can be manipulated to modify, the erythroid phenotype in PV.**

Polycythemia vera (PV) is a myeloproliferative neoplasm driven by activating mutations in *JAK2* that result in unrestrained erythrocyte production, increasing patients' hematocrit and hemoglobin concentrations, placing them at risk of life-threatening thrombotic events. Our genome-wide association study of 440 PV cases and 403 351 controls using UK Biobank data showed that single nucleotide polymorphisms in *HFE* known to cause hemochromatosis are highly associated with PV diagnosis, linking iron regulation to PV. Analysis of the FinnGen dataset independently confirmed overrepresentation of homozygous *HFE* variants in patients with PV. *HFE* influences the expression of hepcidin, the master regulator of systemic iron homeostasis. Through genetic dissection of mouse models of PV, we show that the PV erythroid phenotype is directly linked to hepcidin expression: endogenous hepcidin upregulation alleviates erythroid disease whereas

hepcidin ablation worsens it. Furthermore, we demonstrate that in PV, hepcidin is not regulated by expanded erythropoiesis but is likely governed by inflammatory cytokines signaling via GP130-coupled receptors. These findings have important implications for understanding the pathophysiology of PV and offer new therapeutic strategies for this disease.

Introduction

Polycythemia vera (PV) is a Philadelphia chromosome–negative myeloproliferative neoplasm (MPN) driven by activating mutations in *JAK2*^{1–4} that cause unrestrained erythrocyte production, increasing patients' hematocrit and hemoglobin concentrations. In PV, >95% of cases harbor the *JAK2* V617F mutation, with the remainder of cases usually exhibiting a mutation in *JAK2* exon 12.^{5,6} Complications of elevated hematocrit include venous and arterial thrombosis, and systemic symptoms including headache, visual disturbances, and pruritis.⁷ Therapy typically includes regular venesection to maintain hematocrit below 45%.^{6,8} This phase of the disease may continue for years before some patients develop fibrotic or leukemic transformation.

Iron availability for erythropoiesis (and other tissues) is governed by hepcidin, the master regulator of systemic iron homeostasis.

Hepcidin is produced by the liver and occludes and internalizes the sole cellular iron exporter, ferroportin,^{9,10} preventing recycled iron in macrophages and dietary iron absorbed in the intestine from reaching the plasma and, hence, the bone marrow (BM).¹¹ Elevated hepcidin thus reduces iron availability, whereas suppressed hepcidin enhances it.¹² Systemic iron homeostasis is maintained via the transcriptional regulation of hepcidin, through which iron loading upregulates transcription via the canonical bone morphogenetic protein (BMP)–Suppressor of Mothers against Decapentaplegic (SMAD) signaling pathway.¹³ Hepcidin transcription is suppressed by iron deficiency, partly via matrilysin-2 (encoded by *TMPRSS6*) mediated downregulation of hemojuvelin, a coreceptor for BMP signaling. Increased erythropoiesis also suppresses hepcidin via the erythroid-secreted hormone erythropoietin (EPO),¹⁴ which acts to inhibit BMP signaling.¹⁵ Hepcidin is also upregulated by inflammation¹⁶ (via interleukin-6 [IL-6]–driven JAK–STAT signaling¹⁷).

Systemic iron metabolism and PV may be closely intertwined.¹⁸ Most patients with PV present with iron deficiency at diagnosis.¹⁹ Overt iron deficiency may mask the elevated hemoglobin associated with PV.²⁰ Venesection induces iron deficiency to limit further erythropoiesis. Recent reports have indicated that treatment of patients with PV with hepcidin analogues²¹ or pharmaceutical upregulation of hepcidin in preclinical models of PV^{22,23} may ameliorate disease phenotype. Given emerging interest in the manipulation of iron homeostasis in PV, comprehensive characterization of hepcidin regulation and its role in PV disease is imperative.

Here, we establish and validate an association between disordered systemic iron homeostasis and the risk of PV diagnosis through unbiased genome-wide association studies (GWASs) and evaluate the iron phenotype in a large cohort of patients with PV. We then show that hepcidin levels are critical for governing the severity of the erythroid phenotype using preclinical models of Jak2-V617F-driven PV. Furthermore, we demonstrate that in PV, hepcidin is not downregulated by erythroferone. We also demonstrate an inflammatory phenotype in PV that may influence hepcidin through GP130-coupled receptors. These findings provide novel insights into understanding the pathophysiology of PV and have important implications for new therapeutic interventions.

Methods

Complete details are available in the supplemental Materials, available on the *Blood* website.

Ethics

Patient samples were collected in accordance with Walter and Eliza Hall Institute ethics 18/10LR or were derived from the Cambridge Blood and Stem Cell Biobank under ethics approval 18/EE/0199 (East of England, Cambridge East Research Ethics Committee). All participants provided written informed consent. The UK Biobank has approval from the UK North West Multi-centre Research Ethics Committee as a Research Tissue Bank (approval 21/NW/0157). Use of mice was in accordance with requirements set out by Walter and Eliza Hall Institute Animal Ethics Committee (approvals 2017.031 and 2020.034).

UK biobank GWAS

We undertook a GWAS of PV cases vs controls. Associations with single nucleotide polymorphisms (SNPs) and small indels were tested genome-wide, using regenie,²⁴ per an additive genetic model. Associations included adjustment for sex, age, genotyping array, 10 ancestry principal components, and relatedness. GWAS results were filtered to include only variants with a minor allele frequency of $\geq 1.2\%$. For variants within the *HFE* locus, associations with PV were also tested assuming a recessive model, with covariate adjustment as described earlier. Associations at this locus and the 4 blood cell traits were tested separately in PV cases and controls, using regenie, as described earlier, under both the additive and recessive models.

FinnGen GWAS analysis

We used the FinnGen resource, data release 6.^{25,26} PV cases were identified as having a relevant International Classification

of Diseases-8, -9, or -10 code in the hospital discharge register, cause of death register, or cancer register; controls were individuals without PV without a record of cancer. Genome-wide associations with PV were carried out with adjustment for sex, age, 10 ancestry principal components, and genotyping batch, assuming the use of an additive genetic model. The difference in the proportion of individuals with a homozygous AA genotype in PV cases vs controls was tested using the Fisher exact test.

Patient samples

We analyzed blood from patients with PV who fulfilled the World Health Organization criteria for PV at the time of diagnosis ($n = 30$) whose treatment either included a history of therapeutic venesection ($n = 16$) or not ($n = 14$); and from healthy controls ($n = 30$). Demographics are presented in supplemental Table 1.

Animals

Erythroferone knockout (*Erfe*-KO)^{14,15,27} and inducible hepcidin knockout (iHamp-KO)²⁸ mice have been described previously. Transgenic mice with a single copy Cre recombinase-dependent *Jak2-V617F* transgene located downstream of the *Col1a1* locus (LSL-*Jak2-V617F*; CreERT2^{T/+}) were generated (full methodology in supplemental Materials). Age- and sex-matched control animals were used in all experiments.

BM transplant model of PV

LSL-*Jak2-V617F*; CreERT2^{T/+} (PV) or LSL-*Jak2-V617F* lacking CreERT2 (control) BM cells were injected IV into lethally irradiated Ly5.1/J (B6.SJL-Ptprca Pepcb/BoyJ) recipient mice. Seven weeks after BM transplantation, mice were given tamoxifen (Sigma; 4.2 mg in 90% corn oil or 10% ethanol) via oral gavage on 2 consecutive days to induce expression of the mutant *Jak2* allele. Complete details are given in supplemental Materials.

Administration of drugs, antibodies, and siRNA

TMPRSS6 small interfering RNA (siRNA; Silence Therapeutics GmbH, Berlin, Germany) comprised a double-stranded 19-mer RNA oligonucleotide targeting human *TMPRSS6*, linked to a GalNAc unit at the 5' end of the sense strand enabling hepatic targeting.²⁹ Nontargeting control (NTC) siRNA complimentary to luciferase RNA was used as the control. *TMPRSS6* and NTC siRNA were diluted in sterile phosphate-buffered saline, and 5 mg/kg was administered via subcutaneous injection every 3 weeks for a total of 3 doses.

Antimouse IL-6 (clone MPF-20F3) or rat immunoglobulin G1κ control antibodies (both made in-house) were administered via intraperitoneal injection every 3 days for a total of 7 doses (500 μg per injection) or daily for 5 consecutive days (200 μg per injection).

Statistical analysis

Sample sizes and statistical tests for each experiment are denoted in the figure legends. Data represents mean \pm standard deviation. Statistical testing was performed using Prism version 9.3.1 (GraphPad Software).

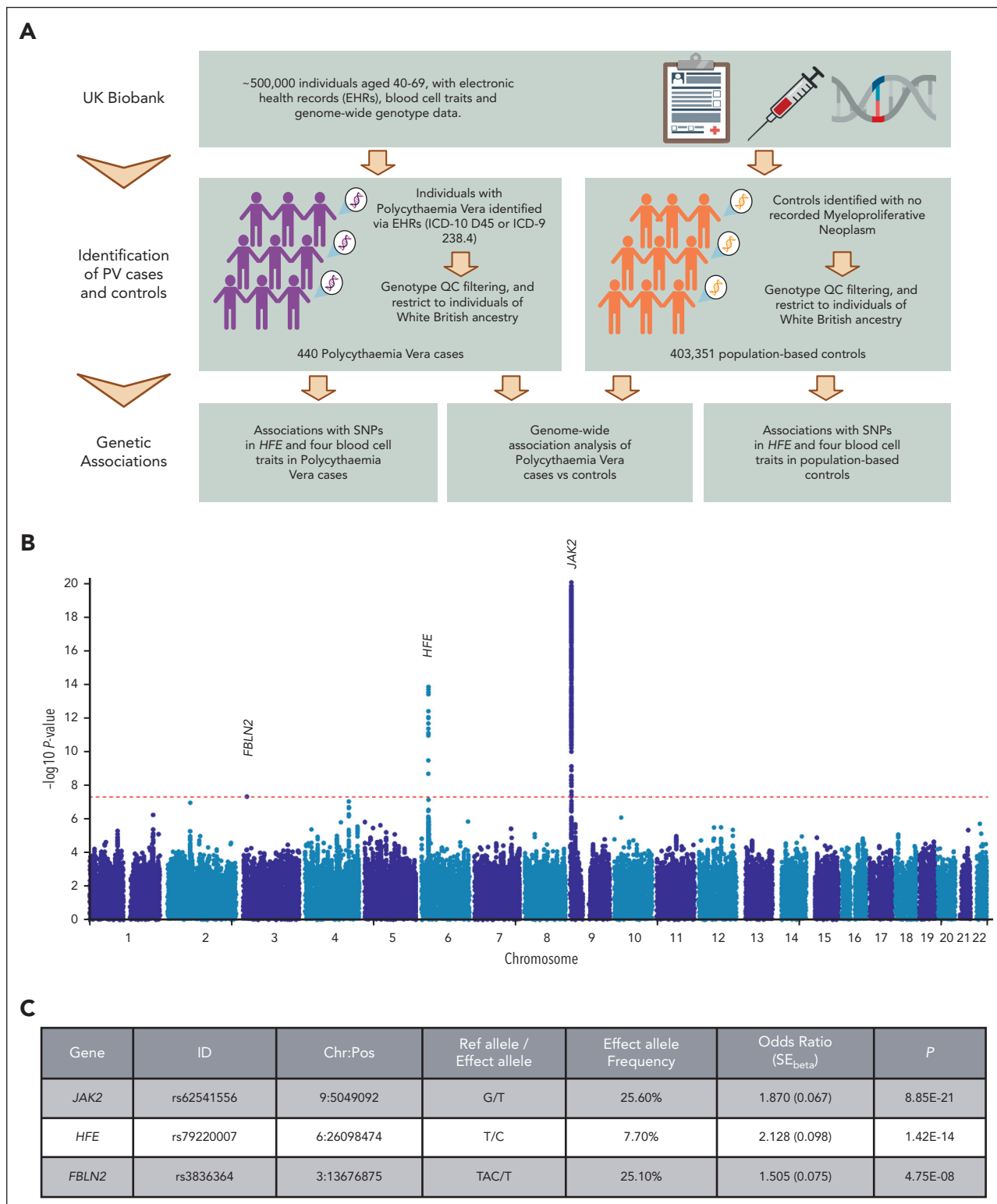


Figure 1. GWAS of PV. (A) Schematic of GWAS. Created with BioRender.com. (B) Manhattan plot showing results of GWAS of 440 PV cases vs 403 351 controls, assuming an additive genetic model. The red dashed line shows genome-wide significance level ($P < 5E-8$). Three loci with associations exceeding this threshold are labeled with the nearest gene. (C) Top SNP at each genetic loci that reached genome-wide significance. (D) LocusZoom plot of associations at the *HFE* locus, assuming a recessive genetic model. Rs1800562 (C282Y) highlighted, with the other SNPs colored per linkage disequilibrium (r^2) to that SNP.

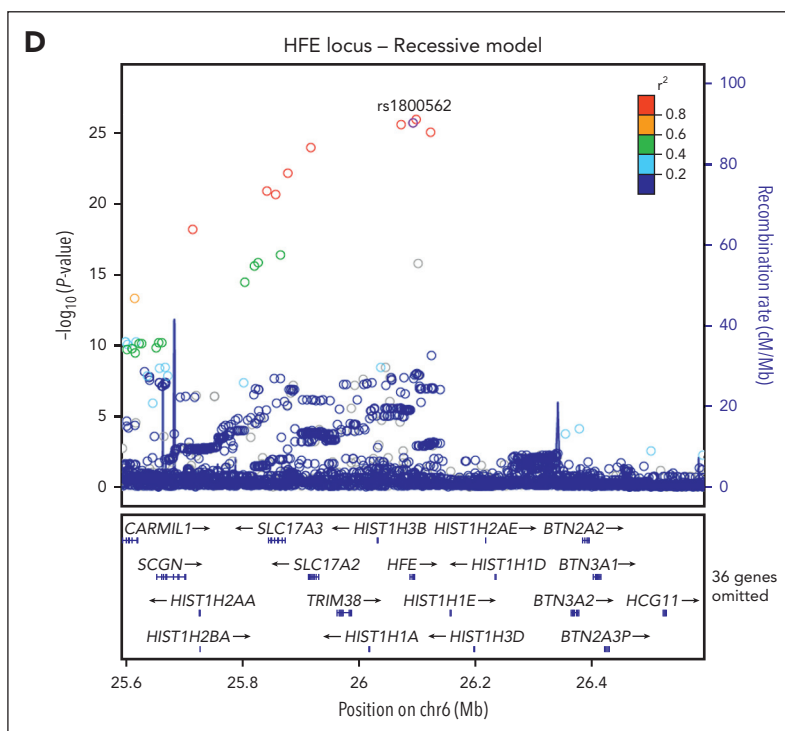


Figure 1 (continued)

Results

GWAS links PV diagnosis with *HFE* variants

We undertook a GWAS of 440 PV cases and 403 351 controls in the UK Biobank (Figure 1A). We tested 9 191 064 variants genome wide (Figure 1B). Three genetic loci had SNPs with genome-wide significant ($P < 5E-8$) associations. Figure 1C details the top SNP at each locus. The most significant association was with rs62541556 ($P = 8.85E-21$), a germ line SNP in *JAK2* that tags the 46/1 haplotype implicated in MPNs and is associated with increased susceptibility to V617F-mutant clonal hematopoiesis.^{30,31} The other genome-wide significant associations were with rs79220007 in *HFE* ($P = 1.42E-14$) and rs3836364 in *FBLN2* ($P = 4.75E-8$).

Interestingly, the top SNP in *HFE*, rs79220007, is in very high linkage disequilibrium ($r^2 = 1.0$) with rs1800562, a SNP known to cause C282Y, the most common mutation causing *HFE*-related hemochromatosis, an autosomal recessive disorder producing iron overload.^{32,33} Among PV cases, there was an excess of individuals with the AA homozygous (C282Y) genotype, compared with the number that would be expected under Hardy-Weinberg equilibrium (2.7 expected vs 35 observed). Given the overrepresentation of AA genotypes in PV cases and the established role of homozygous C282Y variants in disease, we reexamined the *HFE* locus for associations with PV under a recessive model. The association with rs1800562 was more statistically significant under the recessive model than under the additive model ($P = 2.63E-26$ vs $P = 2.91E-14$; supplemental Table 2; Figure 1D), with the homozygous AA genotype associated with a 12.58-times increased odds of PV, compared with G/G or G/A genotypes. Commensurately, there was more than 10-fold increase in the number of individuals with a PV diagnosis for individuals homozygous for C282Y (AA)

($n = 35$, 1.35%, supplemental Table 3), compared with those with GA or GG genotypes ($n = 69$, 0.12%; and $n = 336$, 0.1%, respectively).

Next, we sought confirmation of the association of rs1800562 with PV through a look-up of rs1800562 in a GWAS of PV in the independent FinnGen study (394 PV cases vs 217 902 controls).^{25,26} Again, there was an overrepresentation of the AA genotype among PV cases (0.6 expected vs 4 observed). The crude odds ratio comparing the frequency of the AA homozygous genotype in PV cases vs controls in FinnGen was 5.19 ($P = 8.29E-3$; supplemental Table 4). The FinnGen GWAS assumed an additive genetic model and did not demonstrate an association between rs1800562 and PV ($P = .68$). However, the C282Y variant is less frequent in Finnish than in British populations (minor allele frequency of 3.7% vs 7.8%), therefore, there may have been limited power to capture the recessive association when an additive effect is assumed.

Using the UK Biobank, we then examined associations between rs1800562 and blood cell traits in PV cases and control individuals separately under both additive and recessive models. In line with a previous GWAS,³⁴ in control individuals, the A allele of rs1800562 was highly associated with higher hemoglobin concentrations, hematocrits, and mean corpuscular volume but lower erythrocyte count (supplemental Table 5) compared with those with PV; this latter association was larger and more statistically significant under a recessive model (supplemental Table 5).

HFE regulates iron homeostasis by influencing transcription of hepcidin.³⁵ *HFE* knockout mice exhibit marked reductions in liver *Hamp1* messenger RNA (mRNA) expression.³⁶ The C282Y

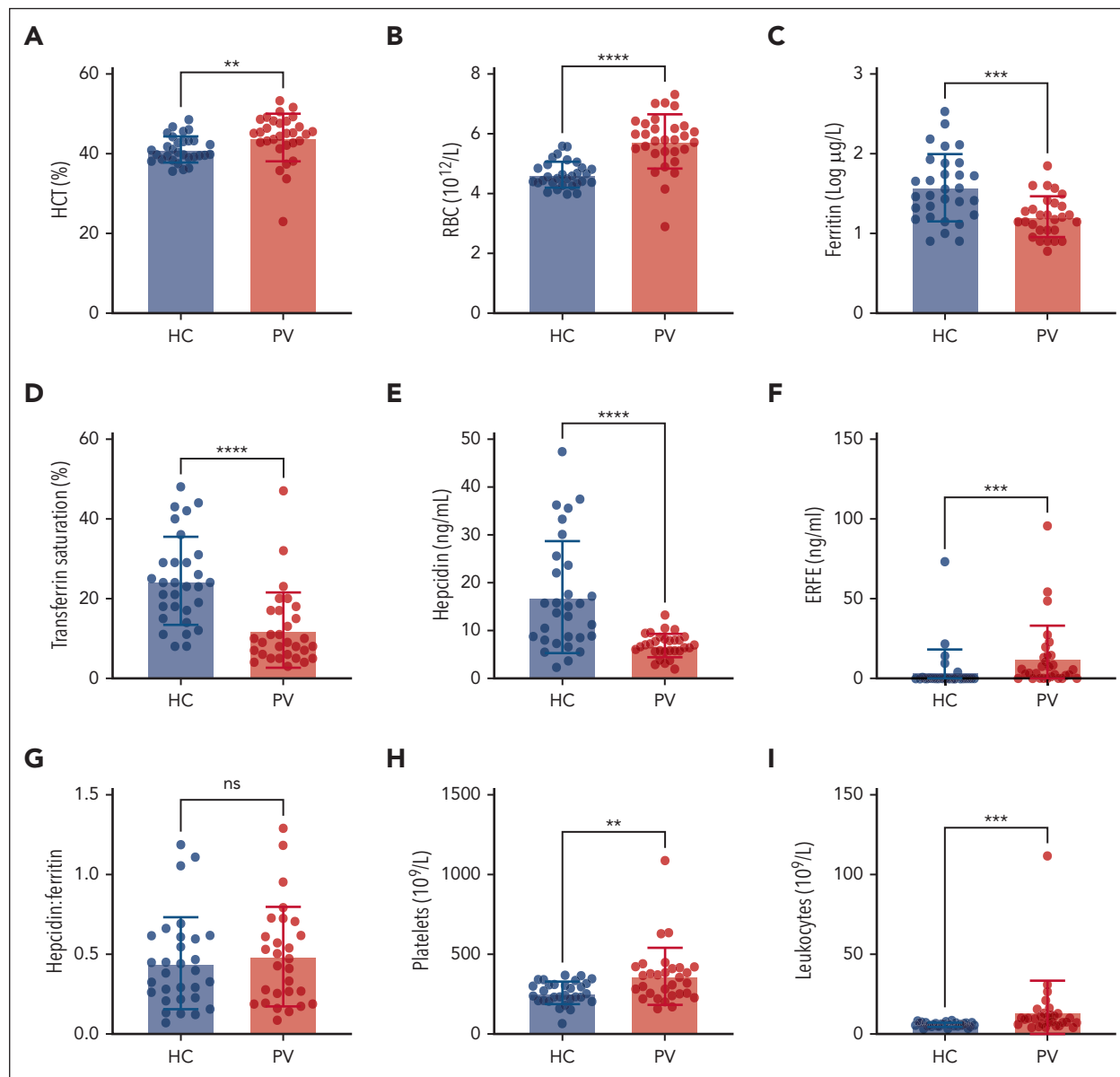


Figure 2. Iron and erythroid parameters in patients with PV and healthy controls. HCT (A), red blood cells (RBCs) (B), ferritin (C), transferrin saturation (D), serum hepcidin (E), serum ERFE (F), hepcidin-to-ferritin ratio (G), platelet count (H), and leukocyte count (I) of healthy controls (HC; blue) and patients with PV (red) (PV and HC, n = 30 each). Mann-Whitney test for panels A,D-I or unpaired 2-tailed t test with Welch correction for panels B-C. ** $P < .01$; *** $P < .001$; **** $P < .0001$. HCT, hematocrit; ns, nonsignificant.

HFE variant dysregulates the iron-hepcidin axis, causing lower hepcidin concentrations relative to iron stores.³⁷ We therefore sought to further investigate how iron homeostasis may affect PV disease.

Patients with PV exhibit iron deficiency with appropriate reductions in hepcidin expression

We compared hematology and iron markers in 30 patients with PV with 30 healthy controls (Figure 2). Patients with PV exhibited increased hematocrit and red cell count, and reduced ferritin (log ferritin: PV, 1.211 vs control, 1.572; $P = .0002$) and transferrin saturation (PV, 12.1% vs control, 24.43%; $P < .0001$); hepcidin levels were reduced (PV, 6.89 ng/mL vs control, 17.01 ng/mL; $P < .0001$), and erythroferrone levels increased (PV, 12.41 ng/mL vs control, 4.26 ng/mL; $P = .0004$). The ratio of

hepcidin-to-ferritin was similar between groups (PV, 0.485 vs control, 0.443; $P = .6048$). As expected, patients with PV had elevated platelet and leukocyte counts. Interestingly, we did not observe significant differences between patients whose treatment included a history of therapeutic venesection and those whose did not (supplemental Figure 1).

Hepcidin regulation in a murine inducible knockin BM transplant model of PV

To define hepcidin regulation in PV, we developed a BM transplant model of PV (Figure 3A). Importantly, this model allows inducible mutant *Jak2-V617F* expression in the hematopoietic lineage while preserving wildtype JAK2-STAT signaling in hepatocytes. Reconstitution of the BM by donor cells was highly efficient (supplemental Figure 2). Ten weeks

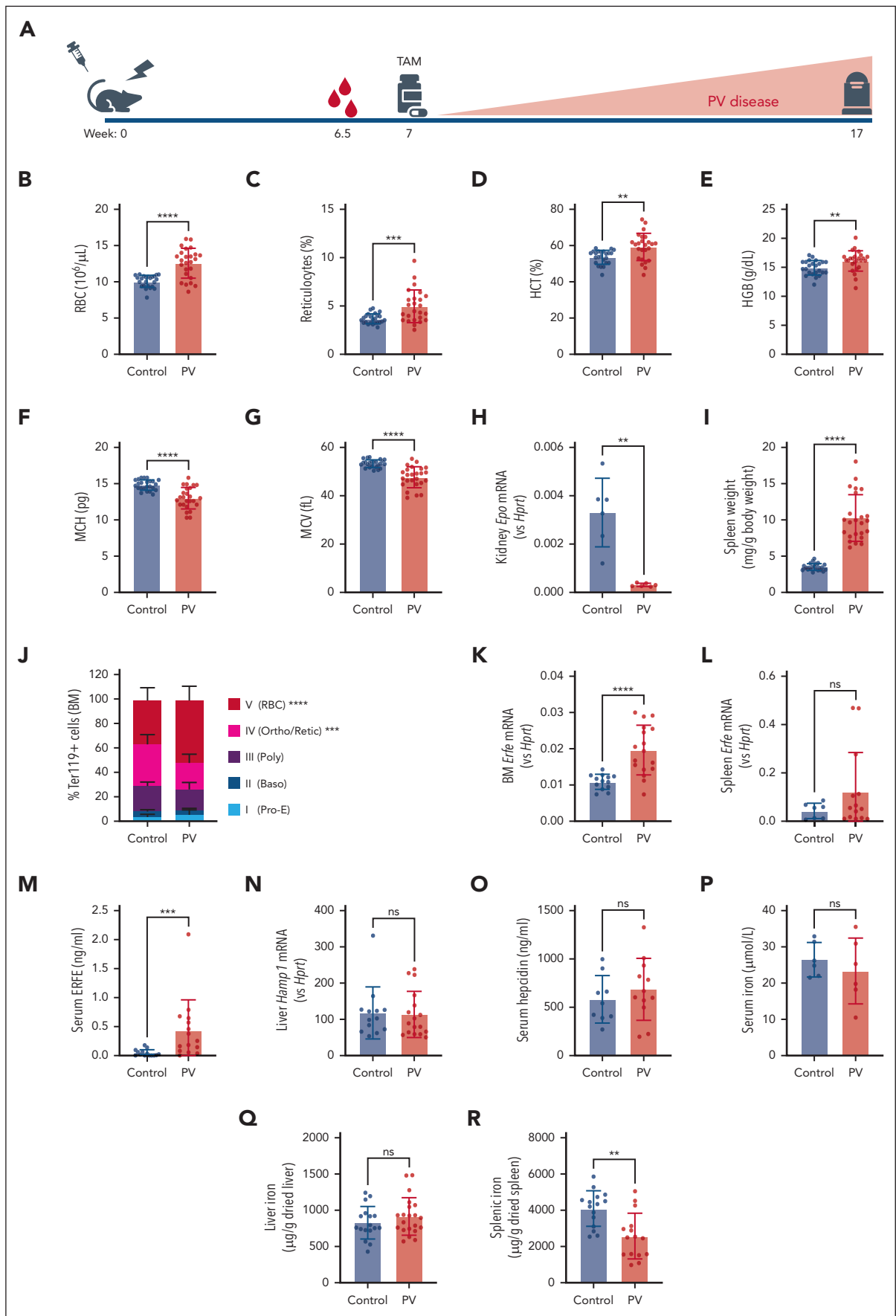


Figure 3.

after tamoxifen induction, recipient mice that received transplantation with LSL-Jak2-V617F; CreERT2^{T/+} BM (hereafter, termed as mice with PV) exhibited a classic PV phenotype with elevated red cell count, reticulocytes, hematocrit and hemoglobin levels; decreased mean corpuscular hemoglobin (MCH) and mean cell volume (MCV); suppressed renal erythropoietin (*Epo*) expression; and splenomegaly (Figure 3B-I); the severity of the phenotype was not inconsistent with human disease. Unlike other murine models of PV,^{38,39} mice with PV did not have thrombocytosis and exhibited only an approximate twofold increase in leukocytes (supplemental Figure 3). Compared with controls, mice with PV had a skewed distribution of BM-resident erythropoietic progenitor cells, with increased levels of the most-mature (stage V) erythroid cells (Figure 3J; supplemental Figure 4). However, in the spleen, erythropoiesis was skewed toward increased intermediate progenitors and reduced stage V cells (supplemental Figure 4). In this PV model, despite increased erythropoiesis and higher *Erfe* mRNA in the BM (but not the spleen) and serum ERFE protein levels (Figure 3K-M), hepcidin mRNA (gene: *Hamp1*) and serum protein levels were not reduced (Figure 3N-O). Serum and liver iron concentrations were similar between mice with PV and controls (Figure 3P-Q), but spleen iron was reduced (Figure 3R).

ERFE does not regulate hepcidin expression in PV

ERFE levels were modestly increased in our PV model (Figure 3M), a magnitude of increase not dissimilar to the clinical cohort (Figure 2F). To determine the effect of ERFE on hepcidin levels and disease severity in PV, we crossbred the LSL-Jak2-V617F; CreERT2^{T/+} mice with a previously generated *Erfe*-KO mouse^{15,27,40} (PV × *Erfe*-KO mice). The intercrossed mice were used as donors for BM transplants, allowing for *Jak2*-V617F expression along with *Erfe* deletion in hematopoietic cells of recipient mice. Although mice with PV have increased ERFE (Figure 3M), ERFE is undetectable in PV × *Erfe*-KO mice (Figure 4A); however, deletion of *Erfe* in mice with PV did not alter hepatic *Hamp1* expression (Figure 4B) or hepcidin protein (Figure 4C) or alter systemic iron levels (Figure 4D-E), erythroid parameters (red cell count, hematocrit, or hemoglobin; Figure 4F-H), terminal erythropoiesis in the BM (Figure 4I), splenomegaly, or other nonerythroid hematologic lineages (supplemental Figure 5).

Hepcidin determines PV erythroid disease severity

We hypothesized that hepcidin regulates erythroid disease in PV. To test this hypothesis, we first deleted hepcidin in mice with PV using a previously generated iHamp-KO mouse model.²⁸ Because mutant *Jak2*-V617F expression in hepatocytes was not a concern in mice unable to express hepcidin, we crossbred LSL-Jak2-V617F; CreERT2^{T/+} mice with iHamp-KO mice, creating mice with simultaneously inducible systemic mutant *Jak2*-V617F expression and hepcidin deletion (PV × iHamp-KO).

As expected, PV × iHamp-KO mice showed no hepatic *Hamp1* expression (Figure 5A) and greatly reduced serum hepcidin protein (Figure 5B). Deletion of hepcidin in mice with PV worsened the erythroid phenotype in PV × iHamp-KO animals, compared with mice with PV that express hepcidin (PV animals), having increased the hemoglobin concentration (19.20 vs 22.70 g/dL; $P = .0021$; Figure 5C), MCH (12.28 vs 17.07 pg; $P < .0001$; Figure 5D), and hematocrit (68.70% vs 75.85%; $P = .0065$; Figure 5E) but did not affect non-erythroid lineages (supplemental Figure 6). Interestingly, hepcidin deletion did not significantly alter the distribution of erythropoietic cells in the BM (Figure 5F). However, the worsened erythroid phenotype may reflect increased iron availability for red cell production as evidenced by increased MCV (43.98 vs 57.62 fL; $P = .0012$; Figure 5G) and increased liver iron (Figure 5H) but did not change the spleen iron content (Figure 5I). PV × iHamp-KO mice had lower red cell counts than the hepcidin-expressing controls ($15.78 \times 10^6/\mu\text{L}$ vs $13.16 \times 10^6/\mu\text{L}$; $P = .0052$; Figure 5J), which, interestingly, recapitulates blood cell traits among controls with the *HFE* rs1800562 A allele (supplemental Table 5). Hepcidin deletion did not affect splenomegaly of mice with PV (supplemental Figure 6).

TMPRSS6 inhibition increases endogenous hepcidin and improves PV disease

Because hepcidin ablation worsened the PV erythroid phenotype, we hypothesized that increasing hepcidin levels would impair erythroid iron availability and reduce erythroid disease. Mice were injected with *TMPRSS6* siRNA (which has been shown to cause sustained knockdown of murine *Tmprss6*²⁹) or NTC siRNA every 3 weeks for a total of 3 injections starting 1 week after tamoxifen induction of the mutant *Jak2*-V617F (Figure 6A), at which time mice with PV had a MPN phenotype (supplemental Figure 7). *TMPRSS6* siRNA treatment resulted in efficient knockdown of hepatic *Tmprss6* (Figure 6B). In mice with PV, compared with NTC siRNA treatment, *TMPRSS6* siRNA increased hepatic *Hamp1* 2.07-fold (Figure 6C) and hepcidin protein 3.10-fold (Figure 6D).

Hepcidin upregulation by *TMPRSS6* siRNA significantly reduced the hematocrit (61.24% vs 43.24%; $P < .0001$; Figure 6E), hemoglobin (17.34 vs 11.35 g/dL; $P < .0001$; Figure 6F), and MCH (13.29 vs 9.84 pg; $P = .0010$; Figure 6G) levels in mice with PV but did not reduce red blood cells ($12.83 \times 10^6/\mu\text{L}$ vs $11.81 \times 10^6/\mu\text{L}$; $P = .1458$; Figure 6H) and had no effect on non-erythroid lineages (supplemental Figure 8). *TMPRSS6* siRNA treatment corrected renal *Epo* suppression (Figure 6I) and the distribution of BM (but not splenic) resident erythropoietic progenitor cells in mice with PV (Figure 6J-K) but had no effect on splenomegaly (supplemental Figure 8). *TMPRSS6* siRNA treatment elevated *Erfe* mRNA expression in the spleen of mice with PV but had no effect on *Erfe* mRNA in the BM or ERFE protein levels in the serum

Figure 3. Novel mouse model of PV. (A) Schematic of BM transplant PV mouse model. (B-G) RBCs (B), reticulocytes (C), HCT (D), HGB (E), MCH (F), and MCV (G); control, n = 24 control and PV, n = 25. (H) Kidney *Epo* mRNA expression relative to *Hprt*; n = 6. (I) Spleen weight normalized to total body weight; n = 24. (J) Terminal erythropoiesis in the BM determined by flow cytometry. Based on CD44 expression and FSC-A, Ter119⁺ cells were gated into 5 distinct populations: I, proerythroblast (Pro-E); II, basophilic erythroblasts (Baso); III, polychromatic erythroblasts (Poly); IV, orthochromatic erythroblasts and reticulocytes (Ortho/Retic); and V, RBCs. Control, n = 24 control and PV, n = 25. *Erfe* mRNA expression relative to *Hprt* in (K) the BM, n = 13 control; PV, n = 17, and (L) the spleen; control, n = 7; PV, n = 14. (M) Serum ERFE; control, n = 14; PV, n = 15. (N) Liver *Hamp1* mRNA expression relative to *Hprt*; control, n = 13; PV, n = 17. (O) Serum hepcidin; control, n = 9 and PV, n = 12. (P) Serum iron; n = 6. (Q) Liver; control, n = 17 and PV, n = 21. (R) Spleen (n = 15) nonheme iron content. Mann-Whitney test for panels B,D,I,L,M,N, unpaired 2-tailed t test with Welch correction for panels C,E,H,K,O,R, or two-way analysis of variance (ANOVA) with Sidák correction for multiple comparisons for panel J. ** $P < .01$; *** $P < .001$; and **** $P < .0001$.

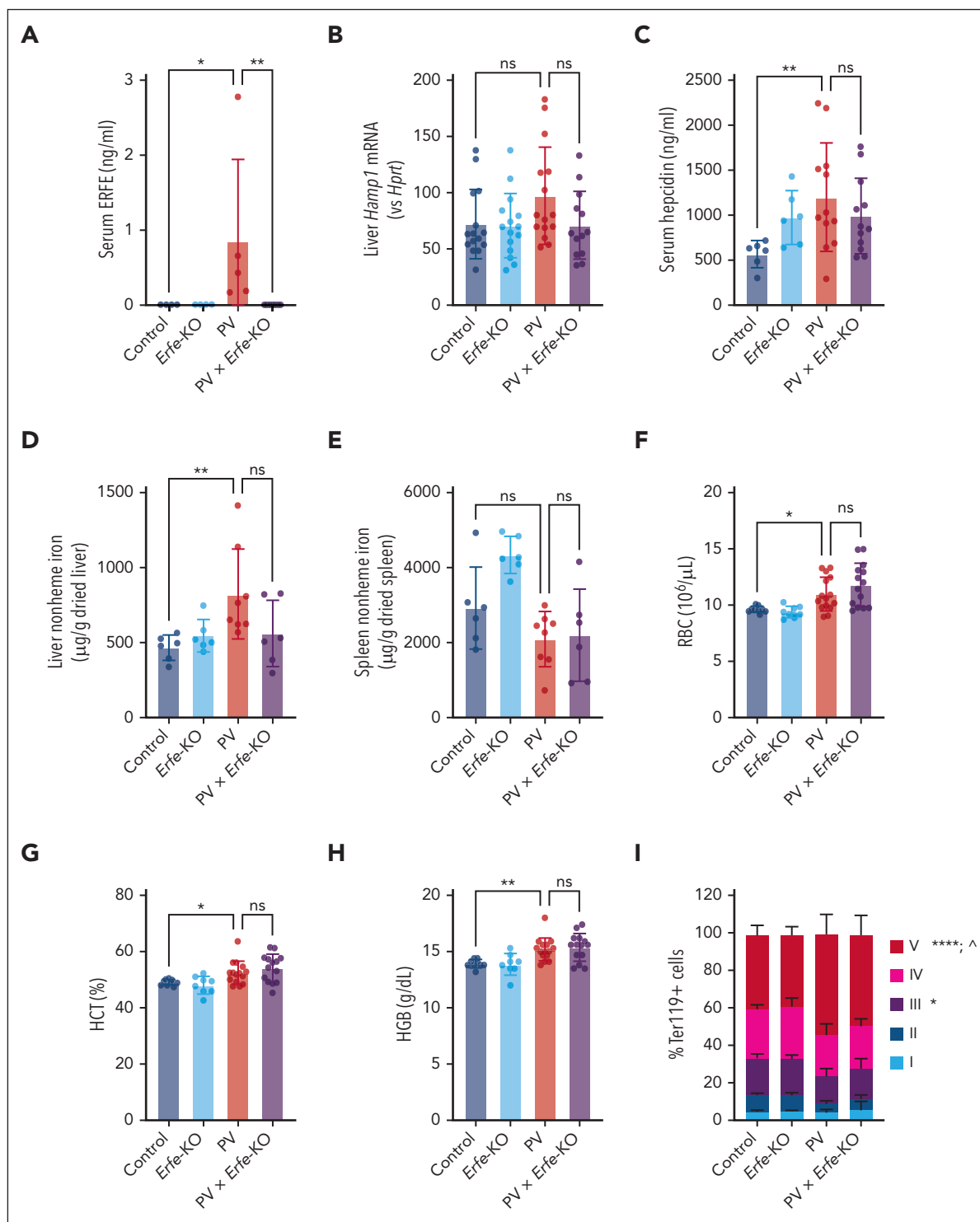


Figure 4. ERFE does not affect hepcidin in PV. (A) Serum ERFE; control, n = 4; *Erfe*-KO, n = 4; PV, n = 5; and PV × *Erfe*-KO, n = 11. (B) Liver *Hamp1* mRNA expression relative to *Hprt*; control, n = 15; *Erfe*-KO, n = 15; PV, n = 15; and PV × *Erfe*-KO, n = 13. (C) Serum hepcidin; control, n = 4; *Erfe*-KO, n = 4; PV, n = 12; and PV × *Erfe*-KO, n = 12. (D) Liver and (E) spleen nonheme iron content; control, n = 6; *Erfe*-KO, n = 6; PV × *Erfe*-KO, n = 6; and PV, n = 8. (F-H) RBCs (F), HCT (G), and HGB (H); control, n = 9; *Erfe*-KO, n = 8; PV, n = 15; and PV × *Erfe*-KO, n = 14. (I) Terminal erythropoiesis in the BM determined by flow cytometry. Based on CD44 expression and FSC-A, Ter119⁺ cells were gated into 5 distinct populations: I, proerythroblast (Pro-E); II, basophilic erythroblasts (Baso); III, polychromatic erythroblasts (Poly); IV, orthochromatic erythroblasts and reticulocytes (Ortho/Retic); and V, RBCs; control, n = 9; *Erfe*-KO, n = 8; PV, n = 13; and PV × *Erfe*-KO, n = 12. One-way ANOVA for panels A,C,E-H, Kruskal-Wallis test for panels B,D, or two-way ANOVA with Dunnett correction for multiple comparisons for panel I. **P* < .05; ***P* < .01; In panel I, “*” represents control vs PV, and “^” represents PV vs PV × *Erfe*-KO.

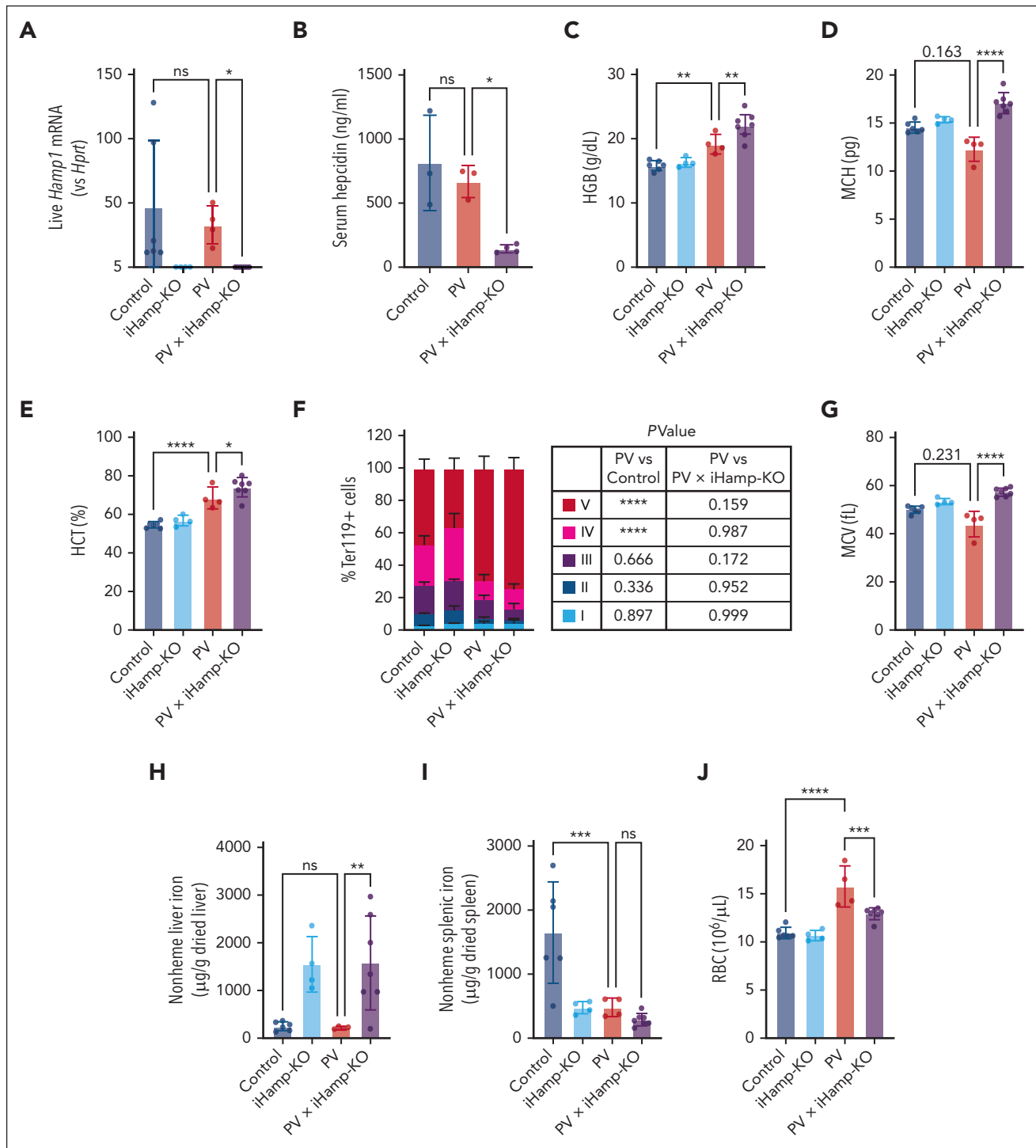


Figure 5. Hepcidin deletion worsens PV erythroid disease severity. (A) Liver *Hamp1* mRNA expression relative to *Hprt*. (B) Serum hepcidin. (C-E) HGB (C), MCH (D), and HCT (E). (F) Terminal erythropoiesis in the BM determined by flow cytometry. Based on CD44 expression and FSC-A, Ter119⁺ cells were gated into 5 distinct populations: I, proerythroblasts; II, basophilic erythroblasts; III, polychromatic erythroblasts; IV, orthochromatic erythroblasts and reticulocytes; and V, RBCs. (G) MCV. (H) Liver and (I) spleen nonheme liver iron. (J) RBCs. Control, n = 6; iHamp-KO, n = 4; PV, n = 4; and PV × iHamp-KO, n = 7, except for panel B in which control, n = 3; PV, n = 3; and PV × iHamp-KO, n = 4. Kruskal-Wallis test for panels A,D,G, ordinary one-way ANOVA for panels B-C,E,H-J, or two-way ANOVA with Dunnett correction for multiple comparisons for panel F. **P* < .05; ***P* < .01; ****P* < .001; *****P* < .0001.

(Figure 6L-N). MCV was reduced in mice with PV treated with *TMPRSS6* siRNA (Figure 6O), indicative of iron-restricted erythropoiesis. *TMPRSS6* siRNA significantly reduced serum

iron in mice with PV (Figure 6P) but did not reduce nonheme liver iron (Figure 6Q) and the treatment raised nonheme splenic iron levels (Figure 6R).

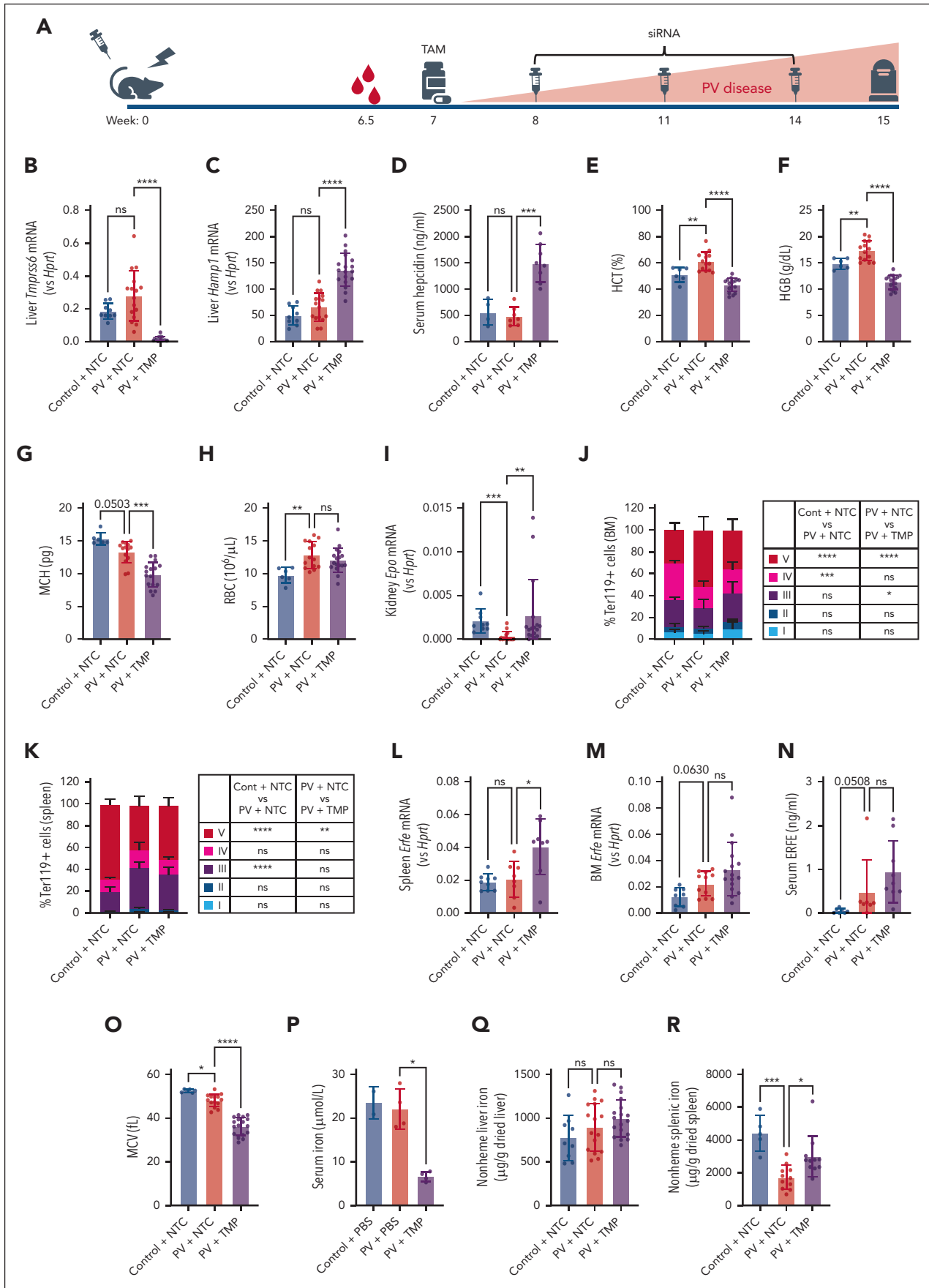


Figure 6.

Inflammatory cytokines may upregulate hepcidin in PV

Inflammatory cytokines (including IL-6) are elevated in PV.^{41,42} Hepcidin transcription is directly regulated via inflammation, via IL-6–mediated JAK-STAT signaling.¹⁷ Thus, we examined whether JAK-STAT signaling was increased in the hepatocytes of mice with PV. RNA-sequencing analysis of livers from animal with PV that received BM transplantation and control animals revealed 1466 differentially expressed genes (DEGs) (598 downregulated; 868 upregulated) (Figure 7A; supplemental Table 6) in mice with PV compared with controls. The transcriptional profile of livers from mice with PV was different from controls (Figure 7B). Gene Ontology pathway analysis of DEGs revealed the upregulation of biological processes related to JAK-STAT signaling in mice with PV compared with control animals (Figure 7C, top 3 bars). Consistent with this analysis, gene set enrichment analysis using the MSigDB hallmark gene sets revealed upregulation of the inflammatory response pathway in the liver of mice with PV (Figure 7C, fourth bar).

Thus, using a human in vitro hepatocyte model, we explored the hypothesis that soluble factors (including cytokines) may upregulate hepcidin in patients with PV. Liver-derived HepG2 cells grown in media supplemented with plasma from patients with PV exhibited increased hepcidin (*HAMP*) mRNA expression compared with cells grown in media supplemented with healthy donor plasma (Figure 7D), indicating that patients with PV produce soluble factors that upregulate hepcidin. We reasoned that IL-6 may be driving this upregulation because mice with PV exhibited increased serum IL-6 (Figure 7E). In addition, RNA-sequencing Gene Ontology pathway analysis as well as gene set enrichment analysis using the MSigDB hallmark gene sets revealed increased IL-6–driven responses in the livers of mice with PV (Figure 7C, fifth to seventh bars). To determine whether IL-6 alone is responsible for hepcidin upregulation in PV, mice that received BM transplantation were treated with anti-IL-6 or control (anti-immunoglobulin G) antibodies. Mice treated with anti-IL-6 antibodies every 3 days for 3 weeks showed normalization of IL6-JAK-STAT (eg, *Saa1*) transcripts and reduced expression of hepatic JAK-STAT transcripts (eg, *Fga*) (Figure 7F-G), confirming neutralization of IL-6 signaling. However, IL-6 neutralization did not alter hepcidin expression (Figure 7H). These results were replicated in mice treated with anti-IL-6 daily for 1 week (supplemental Figure 9). In keeping with unaltered hepcidin expression, anti-IL-6 treatment had a minimal effect on erythropoiesis or iron distribution in mice with PV (supplemental Figure 10).

We therefore hypothesized that other cytokines may upregulate hepcidin in PV. In keeping with this, Kyoto Encyclopedia of

Genes and Genomes (KEGG) pathway analysis of DEGs revealed upregulation of genes involved in cytokine-cytokine receptor interaction in the liver of mice with PV compared with controls (Figure 7C, bottom bar). HepG2 cells cultured in media supplemented with plasma from patients with PV exhibited increased JAK-STAT target gene expression (*Fga*) but no change in BMP-SMAD target gene expression (*SMAD7*) when compared with cells cultured in media supplemented with plasma from healthy donors (Figure 7I). Notably, levels of other IL-6–family cytokines (IL11,^{43,44} oncostatin M [OSM]⁴⁵) are known to be elevated in PV. Thus, we screened other IL-6–family cytokines for a role in hepcidin regulation because these cytokines induce JAK-STAT signaling via a common GP130 receptor subunit (except IL-31). Addition of individual IL-6–family cytokines to HepG2 cells revealed that in addition to IL-6, IL-11, OSM, and leukemia inhibitory factor (LIF) increase *HAMP* mRNA levels; whereas IL-27, cardiotrophin 1 (CT-1), and ciliary neurotrophic factor (CNTF) have no effect, and cardiotrophin-like cytokine factor 1 (CLCF1) decreases hepcidin expression (Figure 7J). The increase in hepcidin expression by IL-11, OSM, and LIF (as well as IL-6) was confirmed in a second hepatocyte cell line, Huh7 (Figure 7K). We then determined whether inhibition of GP130 could normalize hepcidin expression in HepG2 cells treated with PV plasma. HepG2 cells grown in media supplemented with PV plasma and anti-GP130 antibodies no longer exhibited increased *HAMP* expression, rather *HAMP* expression decreased, reaching levels indistinguishable from that of cells cultured in media supplemented with control plasma and anti-GP130 antibodies (Figure 7L).

Discussion

Here, we provide population genetic and experimental evidence that diagnosis and clinical features of PV are influenced by systemic iron homeostasis. This work establishes a central role for iron homeostasis in influencing the erythroid phenotype in PV and provides a rationale for the use of therapies that modify iron metabolism to treat this disease.

Our GWAS implicates the *HFE* locus as a key region associated with PV diagnosis, formally linking systemic iron regulation and PV. The top SNP in *HFE* associated with PV is in very high linkage disequilibrium with the pathogenic *HFE* C282Y variant (which causes hemochromatosis). Interestingly, this disease-causing SNP is not associated with diagnosis of other MPNs (essential thrombocythemia and primary myelofibrosis; supplemental Table 7), indicating that iron metabolism is linked to PV exclusively. Provision of iron to PV may worsen hematocrit.⁴⁶ Conversely, as we show, iron deficiency is common among patients with PV¹⁹ and may conceal diagnosis.⁴⁷

Figure 6. *TMPRSS6* inhibition increases endogenous hepcidin and improves PV disease severity. (A) Schematic of experimental design. (B-C) Liver *Tmprss6* (B) and *Hamp1* (C) mRNA expression relative to *Hprt*; control + NTC, n = 9; PV + NTC, n = 16; PV + TMP, n = 18. (D) Serum hepcidin; control + NTC, n = 4; PV + NTC, n = 7; PV + TMP, n = 8. (E-H) HCT (E), HGB (F), MCH (G), and RBCs (H); control + NTC, n = 6; PV + NTC, n = 14; PV + TMP, n = 17. (I) Kidney *Epo* mRNA expression relative to *Hprt*; control + NTC, n = 9; PV + NTC, n = 16; PV + TMP, n = 17. (J-K) Terminal erythropoiesis in the BM (J) and the spleen (K) determined by flow cytometry. Based on CD44 expression and FSC-A, Ter119⁺ cells were gated into 5 distinct populations: I, proerythroblasts; II, basophilic erythroblasts; III, polychromatic erythroblasts; IV, orthochromatic erythroblasts and reticulocytes; and V, RBCs; BM: control + NTC, n = 7; PV + NTC, n = 13; and PV + TMP, n = 19; and spleen: control + NTC, n = 7; PV + NTC, n = 5; and PV + TMP, n = 7. (L-M) Spleen (L) and BM (M) *Erfe* mRNA expression relative to *Hprt*; spleen: control + NTC, n = 9; PV + NTC, n = 8; and PV + TMP, n = 8; BM: control + NTC, n = 8; PV + NTC, n = 11; PV + TMP, n = 16. (N) Serum *ERFE*; control + NTC, n = 7; PV + NTC, n = 7; and PV + TMP, n = 8. (O) MCV; control + NTC, n = 6; PV + NTC, n = 14; and PV + TMP, n = 17. (P) Serum iron; control group, n = 2; PV groups, n = 4. (Q-R) Liver (Q) and spleen (R) nonheme iron content; liver: control + NTC, n = 9; PV + NTC, n = 16; PV + TMP, n = 18; spleen: control + NTC, n = 5 and PV groups, n = 11. Kruskal-Wallis test for panels B,D,G,I,L-N,P,R, ordinary one-way ANOVA for panels C,E-F,H,O,Q, or two-way ANOVA with Tukey correction for multiple comparisons for panels J-K. **P* < .05; ***P* < .01; ****P* < .001; *****P* < .0001. NTC, nontargeting control siRNA; TMP, *TMPRSS6* siRNA.

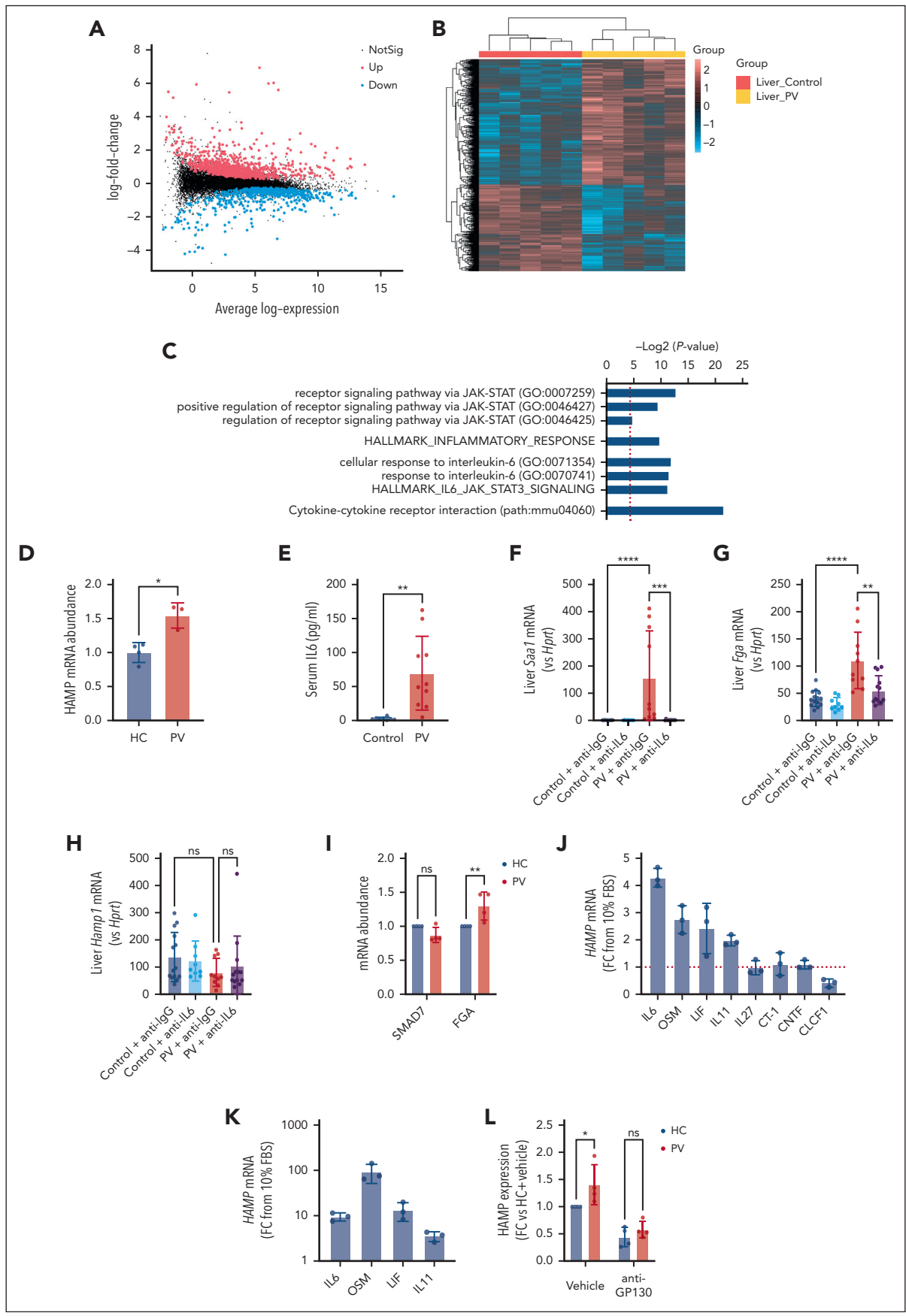


Figure 7.

Previous small studies have examined the prevalence and effects of *HFE* C282Y variants in PV and have not observed associations.^{48,49} However, here, the use of large data sets enabled an unbiased approach to discover and validate the role of *HFE* in PV diagnosis. Cases of PV were defined per the International Classification of Diseases system and subject to contemporaneous criteria at the time of disease diagnosis.

HFE is an upstream regulator of hepcidin, perhaps via stabilization of BMP-type I receptors (ALK3) to facilitate BMP signaling.^{50,51} C282Y variants prevent *HFE* from reaching the cell surface, limiting its function, reducing hepcidin expression, and causing excess iron absorption.^{37,52} *HFE* variants may thus enhance iron availability for erythropoiesis, increasing the likelihood of presentation and diagnosis of PV.

Given the established role of *HFE* in hepcidin regulation, we reasoned that the ultimate mechanism for the genetic association with disease phenotype was via changes in hepcidin, and, hence, we dissected the role of hepcidin in PV using preclinical models. Genetic deletion of hepcidin in our PV model increased erythroid parameters, indicating that in PV, unrestricted erythroid iron access results in unfettered increased hematocrit and hemoglobin production. Conversely, physiologic upregulation of hepcidin expression through RNA interference of *Tmprss6* induced reductions in serum iron, depriving the BM of iron and causing reduced hematocrit and hemoglobin concentrations. Hepcidin is thus critical in determining the erythroid phenotype in PV.

The dependence of the PV erythroid phenotype on systemic iron homeostasis provides the mechanistic rationale for the suite of emerging treatments that target iron metabolism for PV. The mainstay of current treatment for PV is venesection to decrease hematocrit below 45%, at which point serious thrombotic events become less likely.^{8,53} Venesection lowers the hematocrit by removing red blood cells and inducing systemic iron deficiency,¹⁸ thus ameliorating further erythrocyte production.⁵³ However, venesection can cause unwanted adverse effects including vasovagal reactions due to fluid shifts,⁵⁴ as well as symptoms such as chronic fatigue due to systemic iron deficiency,⁵⁵ and incurs direct and indirect health care costs associated with patient visits. Some patients are unable to tolerate venesection because of the severity of adverse events, or do not achieve satisfactory hematocrit responses and, hence, require second-line nontargeted agents. New therapeutic options for PV are thus needed. Withholding iron from the BM by inhibiting iron export to the plasma offers an exciting therapeutic opportunity to replace therapeutic venesection to treat PV.⁵⁶ We

demonstrated that upregulation of endogenous hepcidin levels through liver-specific *TMPRSS6* siRNA deprives the serum of iron and reduces hematocrit and hemoglobin concentrations in our PV model. A similar approach using antisense oligonucleotide therapies has likewise recently shown promising preclinical results.²² A phase 2 clinical trial showed that a hepcidin mimetic can obviate the need for venesection in patients with PV previously dependent on venesection.²¹ A clinical candidate of the *TMPRSS6* siRNA used here (SLN124) is entering phase 1 and 2 clinical trials (NCT05499013) in patients with PV. Our data indicate that liver iron stores were not altered by *TMPRSS6* siRNA treatment but splenic iron stores increased, consistent with this therapy redistributing iron stores rather than inducing systemic iron depletion, a feature that could protect patients from symptomatic iron deficiency. *TMPRSS6* siRNA treatment is unlikely to result in vasovagal responses. Because hepcidin mimetics and *TMPRSS6* siRNA therapies can be administered by subcutaneous injection, these therapies could potentially be self-administered, reducing health care costs.

In our clinical study, we found that patients exhibit low iron stores with concordant reductions in hepcidin that are not likely influenced by small increases in ERFE. Iron depletion and low iron stores have been observed in some previous studies^{18,57} although others have reported hepcidin levels similar to healthy controls.^{58,59} Although we detected elevated ERFE in our PV model and patients with PV, *Erfe* deletion did not modify hepcidin expression or alter disease phenotype. These findings may reflect the smaller degree of ERFE elevation in PV compared with diseases of ineffective erythropoiesis such as thalassemia.⁴⁰ In keeping with this, we found that hepcidin-to-ferritin ratios are not reduced in patients with PV, unlike in thalassemia in which ratios are lower.⁶⁰ Elevations of ERFE in our PV model were comparable with elevations detected in experimental mice with low-level ERFE overexpression, which do not alter hepcidin expression and produce only modest elevations in serum and liver iron.⁶¹

Numerous inflammatory cytokines (including IL-6) are elevated in patients with PV, some of which may portend inferior prognosis.^{42,44,62} We found preliminary evidence to suggest that IL-6–family cytokines (beyond IL-6 itself), which signal via GP130-coupled receptors,⁶³ may be implicated in hepcidin regulation in PV. Consistent with our data, previous studies have indicated that anti-IL-6 treatment of mice with PV does not alter hematologic phenotype.⁶⁴ Further characterization of the role of these cytokine(s) in hepcidin regulation in PV will be an important continuation of this work.

Figure 7. Inflammatory cytokines may upregulate hepcidin in PV. (A) Mean-difference plot showing the average log expression of each gene (x-axis) and their log-fold change between PV and control liver samples (y-axis). The DEGs are highlighted with points in red and blue indicating upregulated and downregulated genes, respectively (adjusted *P* value <.05). (B) Heatmap of the expression of all DEGs with hierarchical clustering in which expression values are standardized to have mean of 0 and standard deviation of 1 for each gene. (C) Bar chart depicting GO biological processes, MSigDB hallmark gene sets, or KEGG pathways relating to JAK-STAT signaling, inflammatory response, IL-6 responses, or cytokine-cytokine receptor interactions that are associated with upregulated genes in PV liver samples vs control. x-axis represents statistical significance of the enrichment, increasing from left to right. The red dotted line represents *P* = .05. (D) *HAMP* mRNA expression of HepG2 cells cultured in media supplemented with 2% plasma from HC donors or patients with PV; HC, n = 4; PV, n = 3. (E) Mouse serum IL-6; control, n = 8; PV, n = 10. (F-H) Liver *Saa1* (F), *Fga* (G), and *Hamp1* (H) relative to *Hprt*; control + anti-immunoglobulin G (IgG), n = 14; control + anti-IL-6, n = 9; PV + anti-IgG, n = 10; and PV + anti-IL-6, n = 13. (I) *SMAD7* and *Fga* mRNA expression of HepG2 cells cultured in media supplemented with 2% plasma from HC donors or patients with PV; n = 4. (J-K) *HAMP* mRNA expression of HepG2 (J) or Huh7 (K) cells cultured in media supplemented with 10 ng/mL recombinant human IL-6–family cytokines; n = 3. The red line in panel J indicates *HAMP* expression in the absence of additional cytokines. (L) *HAMP* mRNA expression of HepG2 cells cultured in media supplemented with 2% plasma from HC donors or patients with PV with the addition of anti-GP130 antibodies or vehicle control (phosphate-buffered saline); n = 4. Unpaired 2-tailed t test with Welch correction for panels D-E, Kruskal-Wallis test for panels F-H, or two-way ANOVA with Šidák correction for multiple comparisons for panels I,L. **P* < .05; ***P* < .01; ****P* < .001; *****P* < .0001. GO, gene ontology; OSM, oncostatin M; LIF, leukemia inhibitory factor; CT-1, cardiotrophin 1; CNTF, ciliary neurotrophic factor; CLCF1, cardiotrophin-like cytokine factor.

Characterization of the functional role of hepcidin and erythroferrone in PV was undertaken in a novel knockin inducible *Jak2-V617F* transplant model, with induction of the phenotype by tamoxifen delayed to ensure recovery of the mouse from the toxicity of the transplant procedure, which could itself induce inflammation and perturb hepcidin.⁶⁵ The hematologic and splenic phenotype of this model, and the degree of upregulation of erythroferrone, was consistent with human PV disease although less severe than previous knockin models of *Jak2-V617F* PV, which have exhibited a stronger phenotype, with higher hemoglobin and hematocrit levels and greater degrees of splenomegaly^{22,39,66,67}; these models may exhibit more marked elevations in erythroferrone, and deletion of erythroferrone in these models may induce a change in hepcidin levels and changes in systemic iron physiology. Evaluation of the role of erythroferrone in alternative models of PV remains an ongoing research need.

In summary, our findings implicate systemic iron regulation as a key determinant of the clinical severity of PV and lay the foundation for strategies that modify iron regulation as potential therapeutics for this disease.

Acknowledgments

The authors thank the Walter and Eliza Hall Institute (WEHI) Bioservices facility for husbandry of all animals and assistance with animal experiments, Stephen Wilcox for assistance with sequencing of RNA indexed libraries, and the WEHI Business Development Office and Legal and Licensing Office for support with Material Transfer Agreements. The authors thank Hal Drakesmith and Andrew Armitage for sharing iHamp and *Erfe* knockout mice. The authors thank all the participants who provided samples for this study, and Kelli Grey, Naomi Sprigg, and Fiona Sultana for collecting patient samples. The authors thank their patient consumers with PV, Nathalie Cook, and Anna Steiner for their input and feedback on this work. The authors acknowledge the participants and investigators of the FinnGen study.

This work was supported by the National Health and Medical Research Council (GNT1158696, GNT1159171, GNT1195236, GNT2009047, GNT1058344 and GNT1113577). Work in the ARG laboratory was supported by grants from CRUK, Wellcome, the WBH Foundation, and the Alborada Trust. This research has been conducted using the UK Biobank Resource under Application Number 36610. This work was also made possible through the Victorian State Government Operational Infrastructure Support and Australian Government National Health and Medical Research Council Independent Research Institute Infrastructure Support Scheme.

The contents of this published material are solely the responsibility of the individual authors and do not reflect the views of the National Health and Medical Research Council or funding partners.

Authorship

Contribution: C.B., K.B., A.P.N., and S.-R.P. conceptualized the study; C.B., V.E.J., U.S., A.L.G., S.J.L., E.J.B., A.R.G., W.S.A., M.B., A.P.N., and S.-R.P. designed the research; C.B., V.E.J., A.P., T.H., G.M.-M., K.F., R.A., D.C., and A.B. performed the research; C.B., V.E.J., A.L.G., and C.S.N.L.-W.-S. analyzed the data; and C.B., V.E.J., U.S., R.A., D.C., A.B., W.S.A., M.B., A.P.N., and S.-R.P. wrote the manuscript.

Conflict-of-interest disclosure: U.S. is a full-time employee of Silence Therapeutics GmbH and has stock options. The remaining authors declare no competing financial interests.

ORCID profiles: C.B., 0000-0002-9796-9381; V.E.J., 0000-0002-9758-9784; U.S., 0000-0003-2556-8391; R.A., 0000-0002-1014-0432; A.B., 0000-0003-2581-1718; A.L.G., 0000-0002-8312-8450; C.S.N.L.-W.-S., 0000-0003-0529-0804; S.J.L., 0000-0003-4756-4762; E.J.B., 0000-0002-5946-5238; A.R.G., 0000-0002-9795-0218; M.B., 0000-0001-5132-0774; A.P.N., 0000-0001-9690-0879; S.-R.P., 0000-0002-5502-0434.

Correspondence: Cavan Bennett, Population Health and Immunity Division, Walter and Eliza Hall Institute of Medical Research, 1G Royal Pde, Parkville, VIC 3052, Australia; email: bennett.c@wehi.edu.au; and Sant-Rayn Pasricha, Population Health and Immunity Division, The Walter and Eliza Hall Institute of Medical Research, 1G Royal Pde, Parkville, VIC 3052, Australia; email: pasricha.s@wehi.edu.au.

Footnotes

Submitted 22 April 2022; accepted 8 March 2023; prepublished online on *Blood* First Edition 16 March 2023. <https://doi.org/10.1182/blood.2022016779>.

Data are available on request from the corresponding authors, Cavan Bennett (bennett.c@wehi.edu.au) and Sant-Rayn Pasricha (pasricha.s@wehi.edu.au).

The online version of this article contains a data supplement.

There is a *Blood Commentary* on this article in this issue.

The publication costs of this article were defrayed in part by page charge payment. Therefore, and solely to indicate this fact, this article is hereby marked "advertisement" in accordance with 18 USC section 1734.

REFERENCES

- Baxter EJ, Scott LM, Campbell PJ, et al. Acquired mutation of the tyrosine kinase *JAK2* in human myeloproliferative disorders. *Lancet*. 2005;365(9464):1054-1061.
- James C, Ugo V, Le Couédic JP, et al. A unique clonal *JAK2* mutation leading to constitutive signalling causes polycythaemia vera. *Nature*. 2005;434(7037):1144-1148.
- Levine RL, Wadleigh M, Cools J, et al. Activating mutation in the tyrosine kinase *JAK2* in polycythemia vera, essential thrombocythemia, and myeloid metaplasia with myelofibrosis. *Cancer Cell*. 2005;7(4):387-397.
- Kralovics R, Passamonti F, Buser AS, et al. A gain-of-function mutation of *JAK2* in myeloproliferative disorders. *N Engl J Med*. 2005;352(17):1779-1790.
- McMullin MF, Wilkins BS, Harrison CN. Management of polycythaemia vera: a critical review of current data. *Br J Haematol*. 2016; 172(3):337-349.
- McMullin MF, Harrison CN, Ali S, et al. A guideline for the diagnosis and management of polycythaemia vera. A British Society for Haematology guideline. *Br J Haematol*. 2019;184(2):176-191.
- Siegel FP, Tauscher J, Petrides PE. Aquagenic pruritus in polycythemia vera: characteristics and influence on quality of life in 441 patients. *Am J Hematol*. 2013;88(8): 665-669.
- Marchioli R, Finazzi G, Specchia G, et al. Cardiovascular events and intensity of treatment in polycythemia vera. *N Engl J Med*. 2013;368(1):22-33.
- Nemeth E, Tuttle MS, Powelson J, et al. Hepcidin regulates cellular iron efflux by binding to ferroportin and inducing its internalization. *Science*. 2004;306(5704): 2090-2093.
- Aschemeyer S, Qiao B, Stefanova D, et al. Structure-function analysis of ferroportin defines the binding site and an alternative mechanism of action of hepcidin. *Blood*. 2018;131(8):899-910.
- Muckenthaler MU, Rivella S, Hentze MW, Galy B. A red carpet for iron metabolism. *Cell*. 2017;168(3):344-361.
- Moretti D, Goede JS, Zeder C, et al. Oral iron supplements increase hepcidin and decrease iron absorption from daily or twice-daily doses in iron-depleted young women. *Blood*. 2015;126(17):1981-1989.

13. Corradini E, Meynard D, Wu Q, et al. Serum and liver iron differently regulate the bone morphogenetic protein 6 (BMP6)-SMAD signaling pathway in mice. *Hepatology*. 2011; 54(1):273-284.
14. Kautz L, Jung G, Valore EV, Rivella S, Nemeth E, Ganz T. Identification of erythroferrone as an erythroid regulator of iron metabolism. *Nat Genet*. 2014;46(7): 678-684.
15. Arezes J, Foy N, McHugh K, et al. Erythroferrone inhibits the induction of hepcidin by BMP6. *Blood*. 2018;132(14): 1473-1477.
16. Nemeth E, Valore EV, Territo M, Schiller G, Lichtenstein A, Ganz T. Hepcidin, a putative mediator of anemia of inflammation, is a type II acute-phase protein. *Blood*. 2003;101(7): 2461-2463.
17. Nemeth E, Rivera S, Gabayan V, et al. IL-6 mediates hypoferrinemia of inflammation by inducing the synthesis of the iron regulatory hormone hepcidin. *J Clin Invest*. 2004;113(9): 1271-1276.
18. Ginzburg YZ, Feola M, Zimran E, Varkonyi J, Ganz T, Hoffman R. Dysregulated iron metabolism in polycythemia vera: etiology and consequences. *Leukemia*. 2018;32(10): 2105-2116.
19. Liu D, Xu Z, Zhang P, et al. Iron deficiency in JAK2 exon12 and JAK2-V617F mutated polycythemia vera. *Blood Cancer J*. 2021; 11(9):154.
20. Campbell PJ, Scott LM, Buck G, et al. Definition of subtypes of essential thrombocythaemia and relation to polycythaemia vera based on JAK2 V617F mutation status: a prospective study. *Lancet*. 2005;366(9501):1945-1953.
21. Kremyanskaya M, Ginzburg Y, Kuykendall AT, et al. PTG-300 eliminates the need for therapeutic phlebotomy in both low and high-risk polycythemia vera patients. *Blood*. 2020;136(suppl 1):33-35.
22. Casu C, Liu A, De Rosa G, et al. Tmprss6-ASO as a tool for the treatment of polycythemia vera mice. *PLoS One*. 2021;16(12):e0251995.
23. Casu C, Oikonomidou PR, Chen H, et al. Minihepcidin peptides as disease modifiers in mice affected by β -thalassemia and polycythemia vera. *Blood*. 2016;128(2): 265-276.
24. Mbatchou J, Barnard L, Backman J, et al. Computationally efficient whole-genome regression for quantitative and binary traits. *Nat Genet*. 2021;53(7):1097-1103.
25. FinnGen. Documentation of R6 release. 2022. Accessed 3 July 2022. <https://finngen.gitbook.io/documentation>
26. Kurki MI, Karjalainen J, Palta P, et al. FinnGen: unique genetic insights from combining isolated population and national health register data. *medRxiv*. Preprint posted 6 March 2022. <https://doi.org/10.1101/2022.03.03.22271360>
27. Pasricha SR, Lim PJ, Duarte TL, et al. Hepcidin is regulated by promoter-associated histone acetylation and HDAC3. *Nat Commun*. 2017;8(1):403.
28. Armitage AE, Lim PJ, Frost JN, et al. Induced disruption of the iron-regulatory hormone hepcidin inhibits acute inflammatory hypoferraemia. *J Innate Immun*. 2016;8(5): 517-528.
29. Vadolas J, Ng GZ, Kysenius K, et al. SLN124, a GalNac-siRNA targeting transmembrane serine protease 6, in combination with deferiprone therapy reduces ineffective erythropoiesis and hepatic iron-overload in a mouse model of β -thalassaemia. *Br J Haematol*. 2021;194(1):200-210.
30. Hinds DA, Barnholt KE, Mesa RA, et al. Germ line variants predispose to both JAK2 V617F clonal hematopoiesis and myeloproliferative neoplasms. *Blood*. 2016;128(8):1121-1128.
31. Anelli L, Zagaria A, Specchia G, Albano F. The JAK2 GGCC (46/1) haplotype in myeloproliferative neoplasms: causal or random? *Int J Mol Sci*. 2018;19(4):1152.
32. Brissot P, Pietrangelo A, Adams PC, de Graaff B, McLaren CE, Loreal O. Haemochromatosis. *Nat Rev Dis Primers*. 2018;4:18016.
33. Girelli D, Busti F, Brissot P, Cabantchik I, Muckenthaler MU, Porto G. Hemochromatosis classification: update and recommendations by the BIOIRON Society. *Blood*. 2022;139(20):3018-3029.
34. Astle WJ, Elding H, Jiang T, et al. The allelic landscape of human blood cell trait variation and links to common complex disease. *Cell*. 2016;167(5):1415-1429.e19.
35. Vujić M. Molecular basis of HFE-hemochromatosis. *Front Pharmacol*. 2014;5: 42.
36. Ahmad KA, Ahmann JR, Migas MC, et al. Decreased liver hepcidin expression in the Hfe knockout mouse. *Blood Cells Mol Dis*. 2002;29(3):361-366.
37. van Dijk BAC, Laarakkers CMM, Klaver SM, et al. Serum hepcidin levels are innately low in HFE-related haemochromatosis but differ between C282Y-homozygotes with elevated and normal ferritin levels. *Br J Haematol*. 2008;142(6):979-985.
38. Akada H, Yan D, Zou H, Fiering S, Hutchison RE, Mohi MG. Conditional expression of heterozygous or homozygous Jak2V617F from its endogenous promoter induces a polycythemia vera-like disease. *Blood*. 2010;115(17):3589-3597.
39. Marty C, Lacout C, Martin A, et al. Myeloproliferative neoplasm induced by constitutive expression of JAK2V617F in knock-in mice. *Blood*. 2010;116(5):783-787.
40. Kautz L, Jung G, Du X, et al. Erythroferrone contributes to hepcidin suppression and iron overload in a mouse model of beta-thalassemia. *Blood*. 2015;126(17):2031-2037.
41. Jain A, Deo P, Sachdeva MUS, et al. Aberrant expression of cytokines in polycythemia vera correlate with the risk of thrombosis. *Blood Cells Mol Dis*. 2021;89:102565.
42. Vaidya R, Gangat N, Jimma T, et al. Plasma cytokines in polycythemia vera: phenotypic correlates, prognostic relevance, and comparison with myelofibrosis. *Am J Hematol*. 2012;87(11):1003-1005.
43. Hermouet S, Godard A, Pineau D, et al. Abnormal production of interleukin (IL)-11 and IL-8 in polycythaemia vera. *Cytokine*. 2002;20(4):178-183.
44. Boissinot M, Cleyrat C, Vilaine M, Jacques Y, Corre I, Hermouet S. Anti-inflammatory cytokines hepatocyte growth factor and interleukin-11 are over-expressed in polycythemia vera and contribute to the growth of clonal erythroblasts independently of JAK2V617F. *Oncogene*. 2011;30(8): 990-1001.
45. Hoermann G, Cerny-Reiterer S, Herrmann H, et al. Identification of oncostatin M as a JAK2 V617F-dependent amplifier of cytokine production and bone marrow remodeling in myeloproliferative neoplasms. *Faseb J*. 2012; 26(2):894-906.
46. Mascarenhas J. Is iron supplementation appropriate for someone with an MPN who has iron-deficient anemia? Ask the expert. *Patient Power*. 23 June 2016. Accessed April 2023. <https://www.patientpower.info/myeloproliferative-neoplasms/ask-the-expert/is-iron-supplementation-appropriate-for-someone-with-an-mpn-who-has-iron-deficient-anemia>
47. Kambali S, Taj A. Polycythemia vera masked due to severe iron deficiency anemia. *Hematol Oncol Stem Cell Ther*. 2018;11(1): 38-40.
48. Andrikovics H, Meggyesi N, Szilvasi A, et al. HFE C282Y mutation as a genetic modifier influencing disease susceptibility for chronic myeloproliferative disease. *Cancer Epidemiol Biomarkers Prev*. 2009;18(3): 929-934.
49. Franchini M, de Matteis G, Federici F, Solero P, Veneri D. Analysis of hemochromatosis gene mutations in 52 consecutive patients with polycythemia vera. *Hematology*. 2004;9(5-6):413-414.
50. Wu XG, Wang Y, Wu Q, et al. HFE interacts with the BMP type I receptor ALK3 to regulate hepcidin expression. *Blood*. 2014; 124(8):1335-1343.
51. Traeger L, Enns CA, Krijt J, Steinbicker AU. The hemochromatosis protein HFE signals predominantly via the BMP type I receptor ALK3 in vivo. *Commun Biol*. 2018;1:65.
52. Barton JC, Edwards CQ, Acton RT. HFE gene: structure, function, mutations, and associated iron abnormalities. *Gene*. 2015; 574(2):179-192.
53. Spivak JL. How I treat polycythemia vera. *Blood*. 2019;134(4):341-352.
54. Adams PC, Barton JC. How I treat hemochromatosis. *Blood*. 2010;116(3): 317-325.
55. Rector WG Jr, Fortuin NJ, Conley CL. Non-hematologic effects of chronic iron deficiency. A study of patients with

- polycythemia vera treated solely with venesections. *Medicine (Baltimore)*. 1982; 61(6):382-389.
56. Handa S, Ginzburg Y, Hoffman R, Kremyanskaya M. Hepcidin mimetics in polycythemia vera: resolving the irony of iron deficiency and erythrocytosis. *Curr Opin Hematol*. 2023;30(2):45-52.
 57. Ganz T, Jung G, Naeim A, et al. Immunoassay for human serum erythropoietin. *Blood*. 2017;130(10):1243-1246.
 58. Albayrak C, Tarkun P, Birtaş Ateşoğlu E, et al. The role of hepcidin, GDF15, and mitoferrin-1 in iron metabolism of polycythemia vera and essential thrombocytosis patients. *Turk J Med Sci*. 2019;49(1):74-80.
 59. Tarkun P, Mehtap O, Ateşoğlu EB, Geduk A, Musul MM, Hacıhanefioğlu A. Serum hepcidin and growth differentiation factor-15 (GDF-15) levels in polycythemia vera and essential thrombocytosis. *Eur J Haematol*. 2013;91(3):228-235.
 60. Jones E, Pasricha SR, Allen A, et al. Hepcidin is suppressed by erythropoiesis in hemoglobin E beta-thalassemia and beta-thalassemia trait. *Blood*. 2015;125(5):873-880.
 61. Coffey R, Jung G, Olivera JD, et al. Erythroid overproduction of erythropoietin causes iron overload and developmental abnormalities in mice. *Blood*. 2022;139(3):439-451.
 62. Øbro NF, Grinfeld J, Belmonte M, et al. Longitudinal cytokine profiling identifies GRO- α and EGF as potential biomarkers of disease progression in essential thrombocytosis. *HemaSphere*. 2020;4(3): e371.
 63. Metcalfe RD, Putoczki TL, Griffin MDW. Structural understanding of interleukin 6 family cytokine signaling and targeted therapies: focus on interleukin 11. *Front Immunol*. 2020;11:1424.
 64. Baldauf CK, Muller P, Haage TR, et al. Anti-IL-6 cytokine treatment has no impact on elevated hematocrit or splenomegaly in a polycythemia vera mouse model. *Blood Adv*. 2022;6(2):399-404.
 65. Kanda J, Mizumoto C, Kawabata H, et al. Serum hepcidin level and erythropoietic activity after hematopoietic stem cell transplantation. *Haematologica*. 2008;93(10):1550-1554.
 66. Akada H, Akada S, Gajra A, et al. Efficacy of vorinostat in a murine model of polycythemia vera. *Blood*. 2012;119(16): 3779-3789.
 67. Mullally A, Lane SW, Ball B, et al. Physiological Jak2V617F expression causes a lethal myeloproliferative neoplasm with differential effects on hematopoietic stem and progenitor cells. *Cancer Cell*. 2010;17(6): 584-596.

© 2023 by The American Society of Hematology. Licensed under [Creative Commons Attribution-NonCommercial-NoDerivatives 4.0 International \(CC BY-NC-ND 4.0\)](https://creativecommons.org/licenses/by-nc-nd/4.0/), permitting only noncommercial, nonderivative use with attribution. All other rights reserved.